Characterization of the transcriptome, nucleotide sequence polymorphism, and natural selection in the desert adapted mouse *Peromyscus eremicus*

Matthew D. MacManes[1], Michael B. Eisen [2],

[1] Department of Molecular, Cellular and Biomedical Sciences, University of New Hampshire, Durham NH, USA

[2] HHMI and University of California, Berkeley, Berkeley, CA, USA

∗ E-mail: macmanes@gmail.com, @PeroMHC

1 Abstract

2 As a direct result of intense heat and aridity, deserts are thought to be among the most harsh of
3 environments, particularly for their mammalian inhabitants. Given that osmoregulation can be
4 challenging for these animals, with failure resulting in death, strong selection should be observed
5 on genes related to the maintenance of water and solute balance. One such animal, *Peromyscus*
6 *eremicus*, is native to the desert regions of the southwest United States and may live its entire
7 life without oral fluid intake. As a first step toward understanding the genetics that underlie
8 this phenotype, we present a characterization of the *P. eremicus* transcriptome. We assay four
9 tissues (kidney, liver, brain, testes) from a single individual and supplement this with popu-
10 lation level renal transcriptome sequencing from 15 additional animals. We identified a set of
11 transcripts undergoing both purifying and balancing selection based on estimates of Tajima's
12 D. In addition, we used the branch-site test to identify a transcript -Slc2a9, likely related to
13 desert osmoregulation – undergoing enhanced selection in *P. eremicus* relative to a set of related
14 non-desert rodents.

15

16 Introduction

17 Deserts are widely considered one of the harshest environments on Earth. Animals living in
18 desert environments are forced to endure intense heat and drought, and as a result, species liv-
19 ing in these environments are likely to posses specialized mechanisms to deal with them. While
20 living in deserts likely involves a large number of adaptive traits, the ability to osmoregulate –
21 to maintain the proper water and electrolyte balance – appears to be paramount [1]. Indeed,
22 the maintenance of water balance is one of the most important physiologic processes for all
23 organisms, whether they be desert inhabitants or not. Most animals are exquisitely sensitive
24 to changes in osmolality, with slight derangement eliciting physiologic compromise. When the
25 loss of water exceeds dietary intake, dehydration - and in extreme cases, death - can occur.

26 Thus there has likely been strong selection for mechanisms supporting optimal osmoregulation
27 in species that live where water is limited. Understanding these mechanisms will significantly
28 enhance our understanding of the physiologic processes underlying osmoregulation in extreme
29 environments, which will have implications for studies of human health, conservation, and cli-
30 mate change.

31

32 The genes and structures responsible for the maintenance of water and electrolyte balance
33 are well characterized in model organisms such as mice [2], rats [3–5], and humans [6–8]. These
34 studies, many of which have been enabled by newer sequencing technologies, provide a founda-
35 tion for studies of renal genomics in non-model organisms. Because researchers have long been
36 interested in desert adaptation, a number of studies have looked at the morphology or expression
37 of single genes in the renal tissues of desert adapted rodents *Phyllotis darwini* [9], *Psammomys*
38 *obesus* [10], and *Perognathus penicillatus* [11]. More recently, full renal transcriptomes have
39 been generated for *Dipodomys spectabilis* and *Chaetodipus baileyi*, [12] as well as *Abrothrix oli-*
40 *vacea* [13].

41

42 These studies provide a rich context for current and future work aimed at developing a syn-
43 thetic understanding of the genetic and genomic underpinnings of desert adaptation in rodents.
44 As a first step, we have sequenced, assembled, and characterized the transcriptome (using four
45 tissue types - liver, kidney, testes and brain) of a desert adapted cricetid rodent endemic to the
46 southwest United States [14], *Peromyscus eremicus*. These animals have a lifespan typical of
47 small mammals, and therefore an individual may live its entire life without ever drinking water.
48 These rodents have distinct advantage over other desert animals (e.g. *Dipodomys*) in that they
49 breed readily in captivity, which enables future laboratory studies of the phenotype of interest.
50 In addition, the focal species is positioned in a clade of well known animals (e.g. *P. californicus*,
51 *P. maniculatus*, and *P. polionotus*) [15] with growing genetic and genomic resources [16–18].
52 Together, this suggests that future comparative studies are possible.

53

54 While the elucidation of the mechanisms underlying adaptation to desert survival is beyond
55 the scope of this manuscript, we aim to lay the groundwork by characterizing the transcriptome
56 from four distinct tissues (brain, liver, kidney, testes). These data will be included in the current
57 larger effort aimed at sequencing the entire genome. Further, via sequencing the renal tissue
58 of a total of 15 additional animals, we characterize nucleotide polymorphism and genome-wide
59 patterns of natural selection. Together, these investigations will aid in our overarching goal to
60 understand the genetic basis of adaptation to deserts in *P. eremicus*.

Materials and Methods

Animal Collection and Study Design

To begin to understand how genes may underlie desert adaptation, we collected 16 individuals from a single population of *P. eremicus* over a two-year time period (2012-2013). These individuals were captured in live traps and then euthanized using isoflurane overdose and decapitation. Immediately post-mortem, the abdominal and pelvic organs were removed, cut in half (in the case of the kidneys), placed in RNAlater and flash frozen in liquid Nitrogen. Removal of the brain, with similar preservation techniques, followed. Time from euthanasia to removal of all organs never exceeded five minutes. Samples were transferred to a -80C freezer at a later date. These procedures were approved by the University of California Berkeley Animal Care and Use Committee and followed guidelines established by the American Society of Mammalogy for the use of wild animals in research [19].

RNA extraction and Sequencing

Total RNA was extracted from each tissue using a TRIzol extraction (Invitrogen) following the manufacturer's instructions. Because preparation of an RNA library suitable for sequencing is dependent on having high quality, intact RNA, a small aliquot of each total RNA extract was analyzed on a Bioanalyzer 2100 (Agilent, Palo Alto, CA, USA). Following confirmation of sample quality, the reference sequencing libraries were made using the TruSeq stranded RNA prep kit (Illumina), while an unstranded TruSeq kit was used to construct the other sequencing libraries. A unique index was ligated to each sample to allow for multiplexed sequencing. Reference libraries (n=4 tissue types) were then pooled to contain equimolar quantities of each individual library and submitted for Illumina sequencing using two lanes of 150nt paired end sequencing employing the rapid-mode of the HiSeq 2500 sequencer at The Hubbard Center for Genome Sciences (University of New Hampshire). The remaining 15 libraries were similarly multiplexed and sequenced in a mixture of 100nt paired and single end sequencing runs across several lanes of an Illumina HiSeq 2000 at the Vincent G. Coates Genome Center (University of California, Berkeley).

Sequence Data Preprocessing and Assembly

The raw sequence reads corresponding to the four tissue types were error corrected using the software bless [20] using kmer=25, based on the developer's default recommendations. The error-corrected sequence reads were adapter and quality trimmed following recommendations from MacManes [21] and Mbandi [22]. Specifically, adapter sequence contamination and low

93 quality nucleotides (defined as PHRED <2) were removed using the program Trimmomatic ver-
94 sion 0.32 [23]. Reads from each tissue were assembled using the Trinity version released 17
95 July 2014 [24]. We used flags to indicate the stranded nature of sequencing reads and set the
96 maximum allowable physical distance between read pairs to 999nt. The assembly was con-
97 ducted on a linux workstation with 64 cores and 512Gb RAM. To filter the raw sequence
98 assembly, we downloaded *Mus musculus* cDNA and ncRNA datasets from Ensembl (`ftp:`
99 `//ftp.ensembl.org/pub/release-75/fasta/mus_musculus/`) and the *Peromyscus manicula-*
100 *tus* reference transcriptome from NCBI (`ftp://ftp.ncbi.nlm.nih.gov/genomes/Peromyscus_`
101 `maniculatus_bairdii/RNA/`). We used a blastN procedure (default settings, evalue set to
102 10^{-10}) to identify contigs in the *P. eremicus* dataset likely to be biological in origin. This pro-
103 cedure, when a reference dataset is available, retains more putative transcripts that a strategy
104 employing expression-based filtering (remove if TMP <1 [25]) of the raw assembly. We then
105 concatenated the filtered assemblies from each tissue into a single file and reduced redundancy
106 using the software cd-hit-est [26] using default setting, except that sequences were clustered
107 based on 95% sequence similarity. This multi-fasta file was used for all subsequent analyses,
108 including annotation and mapping.

109

Assembled Sequence Annotation

111 The filtered assemblies were annotated using the default settings of the blastN algorithm [27]
112 against the Ensembl cDNA and ncRNA datasets described above, downloaded on 1 August
113 2014. Among other things, the Ensemble transcript identifiers were used in the analysis of
114 gene ontology conducted in the PANTHER package [28]. Next, because rapidly evolving nu-
115 cleotide sequences may evade detection by blast algorithms, we used HMMER3 [29] to search for
116 conserved protein domains contained in the dataset using the Pfam database [30]. Lastly, we ex-
117 tracted putative coding sequences using Transdecoder version 4Jul2014 (`http://transdecoder.`
118 `sourceforge.net/`)

119

120 To identify patterns of gene expression unique to each tissue type, we mapped sequence reads
121 from each tissue type to the reference assembly using bwa-mem [31]. We estimated expression
122 for the four tissues individually using default settings of the software eXpress [32]. Interesting
123 patterns of expression, including instances where expression was limited to a single tissue type,
124 were identified and visualized.

125

Population Genomics

In addition to the reference individual sequenced at four different tissue types, we sequenced 15 other conspecific individuals from the same population in Palm Desert, California. Sequence data were mapped to the reference transcriptome using bwa-mem. The alignments were sorted and converted to BAM format, then passed to the program ANGSD version 0.610, which was used for calculating the folded site frequency spectrum (SFS) and Tajima's D [33].

Natural Selection

To characterize natural selection on several genes related to water and ion homeostasis, we identified several of the transcripts identified as experiencing positive selection in a recent work on desert-adapter *Dipodomys* rodents. The coding sequences corresponding to these genes, Solute Carrier family 2 member 9 (Slc2a9) and the Vitamin D3 receptor (Vdr), were extracted from the dataset, aligned using the software MACSE [34] to homologous sequences in *Mus musculus*, *Rattus norvegicus*, *Peromyscus maniculatus*, and *Homo sapiens* as identified by the conditional reciprocal best blast procedure (CRBB, [35]). An unrooted gene tree was constructed using the online resource Clustal-Omega, and the tree and alignment were analyzed using the branch-site model (model=2, nsSites=2, fix_omega=0 versus model=2, nsSites=2, fix_omega=1, omega=1) implemented in PAML version 4.8 [36, 37]. Significance was evaluated via the use of the likelihood ratio test.

Results and Discussion

RNA extraction, Sequencing, Assembly, Mapping

RNA was extracted from the hypothalamus, renal medulla, testes, and liver from each individual using sterile technique. TRIzol extraction resulted in a large amount of high quality (RIN $\geq$ 8) total RNA, which was then used as input. Libraries were constructed as per the standard Illumina protocol and sequenced as described above. The number of reads per library varied from 56 million strand-specific paired-end reads in Peer360 kidney, to 9 million single-end reads in Peer321 (Table 1, available on the Short Read Archive accession XXX). Adapter sequence contamination and low-quality nucleotides were eliminated, which resulted in a loss of <2% of the total number of reads. These trimmed reads served as input for all downstream analyses.

Table 1

Dataset	Num. Raw Reads
Peer360 Testes	32M PE/SS
Peer360 Liver	53M PE /SS
Peer360 Kidney	56M PE/SS
Peer360 Brain	23M PE/SS
Peer305	19M PE
Peer308	15M PE
Peer319	14M PE
Peer321	9M SE
Peer340	16M PE
Peer352	14M PE
Peer354	9M SE
Peer359	14M PE
Peer365	16M PE
Peer366	16M PE
Peer368	14M PE
Peer369	14M PE
Peer372	17M SE
Peer373	23M SE
Peer380	16M SE
Peer382	14M SE

Table 1. The number of sequencing reads per sample, indicated by Peer[number]. PE=paired end, SS=strand specific, SE=single end sequencing.

Transcriptome assembly for each tissue type was accomplished using the program Trinity [24]. The raw assembly for brain, liver, testes, and kidney contained 185425, 222096, 180233, and 514091 assembled sequences respectively. This assembly was filtered using a blastN procedure against the *Mus* cDNA and ncRNA and *P. maniculatus* cDNAs, which resulted in a final dataset containing 68331 brain-specific transcripts, 71041 liver-specific transcripts, 67340 testes-specific transcripts, and 113050 kidney-specific transcripts. Mapping the error-corrected adapter/quality trimmed reads to these datasets resulted in mapping 94.98% (87.01% properly paired) of the brain-derived reads to the brain transcriptome, 96.07% (88.13% properly paired) of the liver-derived reads to the liver transcriptome, 96.81% (85.10% properly paired) of the testes-derived reads to the testes transcriptome, and 91.87% (83.77% properly paired) of the kidney-derived reads to the kidney transcriptome. Together, these statistics suggest that the tissue-specific transcriptomes are of extremely high quality. All tissue-specific assemblies are to be made available on Dryad.

174

175   **Figure 1**
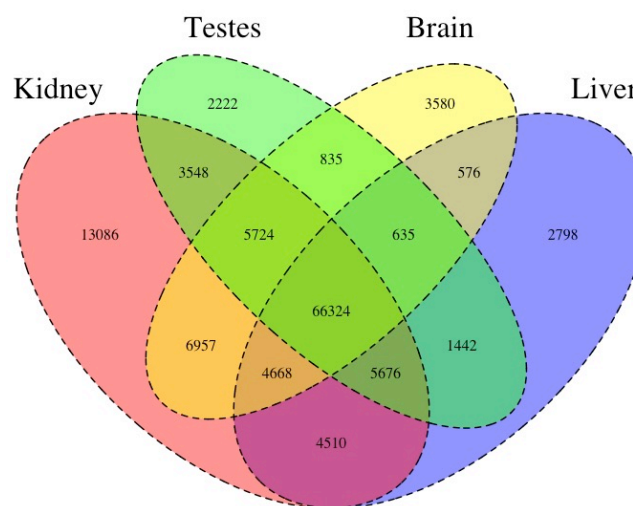
176

177   Figure 1. The Venn Diagram.

178   We then estimated gene expression on each of these tissue-specific datasets, which allowed
179   us to understand expression patterns in the multiple tissues. Specifically, we constructed a Venn
180   diagram (Figure 1) that allowed us to visualize the proportion of genes whose expression was
181   limited to a single tissue and those whose expression was ubiquitous. 66324 transcripts are
182   expressed on all tissue types, while 13086 are uniquely expressed in the kidney, 2222 in the
183   testes, 3580 in the brain, and 2798 in the liver. The kidney appears to an outlier in the number
184   of unique sequences, though this could be the result of the recovery of more lowly expressed
185   transcripts that may be the result of deeper sequencing.

186

187   In addition to this, we estimated mean TMP (number of transcripts per million) for all tran-
188   scripts. Table 2 consists of the 10 genes whose mean TMP was the highest. Several genes in this
189   list are predominately present in a single tissue type. For instance Transcript_126459, Albumin
190   is very highly expressed in the liver, but less so in the other tissues. It should be noted, however,
191   that making inference based on uncorrected values for TPM is not warranted. Statistical testing
192   for differential expression was not implemented due to the fact that no replicates are available.

193

194   After expression estimation, the filtered assemblies were concatenated together, and after
195   the removal of redundancy with cd-hit-est, 123,123 putative transcripts remained (to be made

196 available on Genbank). From this filtered concatenated dataset, we extracted 71626 putative
197 coding sequences (72Mb, to be made available on Dryad). Of these 71626 sequences, 38221 were
198 complete exons (containing both start and stop codons), while the others were either truncated
199 at the 5-prime end (20239 sequences), the 3-prime end (6445 sequences), or were internal (6721
200 sequencing with neither stop nor start codon). The results of a Pfam search conducted on the
201 predicted amino acid sequences will be found on Dryad.

202

203 **Table 2**

204

Transcript ID	Testes	Liver	Kidney	Brain	Genbank ID	Gene ID
Transcript_83842	2.05E+03	6.40E+03	1.03E+04	5.47E+03	DQ073446.1	COX2
Transcript_126459	1.43E+01	2.22E+04	2.77E+01	6.73E+00	XM_006991665.1	Alb
Transcript_128937	4.39E+00	1.91E+04	4.74E+02	2.23E+00	XM_007627625.1	Apoa2
Transcript_81233	1.71E+03	5.23E+03	6.11E+03	3.08E+03	XM_006993867.1	Fth1
Transcript_94125	3.67E+01	1.08E+04	2.09E+03	2.75E+00	XM_006977178.1	CytP450
Transcript_119945	5.03E+03	1.15E+03	1.33E+03	3.71E+03	XM_008686011.1	Ubb
Transcript_5977	4.95E+00	1.01E+04	3.05E+02	3.58E+02	XM_006978668.1	Tf
Transcript_4057	2.62E+01	9.32E+03	1.34E+02	8.38E+01	XM_006994871.1	Apoc1
Transcript_112523	4.07E+02	7.36E+03	7.78E+02	9.54E+02	XM_006994872.1	Apoe
Transcript_98376	1.98E+00	8.66E+03	1.02E+00	2.68E+00	XM_006970208.1	Ttr

206 Table 2. The 10 transcripts with the highest mean TPM (transcripts per million).

Population Genomics

208 As detailed above, RNAseq data from 15 individuals were mapped to the reference transcrip-
209 tome with the resulting BAM files being used as input to the software package ANGSD. The
210 Tajima's D statistic was calculated for all transcripts covered by at least 14 of the 15 individ-
211 uals. In brief, a negative Tajima's D - a result of lower than expected average heterozygosity -
212 is often associated with purifying or directional selection, recent selective sweep or population
213 bottleneck. In contrast, a positive value for Tajima's D represents higher than expected average
214 heterozygosity, often associated with balancing selection.

215

216 The distribution of the estimates of Tajima's D for all of the assembled transcripts is shown
217 in Figure 2. The distribution is skewed toward negative values (mean=-0.89, variance=0.58),
218 which is likely the result of purifying selection, a model of evolution commonly invoked for
219 coding DNA sequences [38]. Table 3 presents the 10 transcripts whose estimate of Tajima's D
220 is the greatest, while Table 4 presents the 10 transcripts whose estimate of Tajima's D is the

221 least. The former list of genes is likely to contain transcripts experiencing balancing selection
222 in the studied population. This list includes, interestingly, genes obviously related to solute
223 and water balance (e.g. Clcnkb and a transmembrane protein gene) and immune function (a
224 interferon-inducible GTPase and a Class 1 MHC gene). The latter group, containing transcripts
225 whose estimates of Tajima's D are the smallest are likely experiencing purifying selection. Many
226 of these transcripts are involved in core regulatory functions where mutation may have strongly
227 negative fitness consequences.

228

229 **Figure 2**
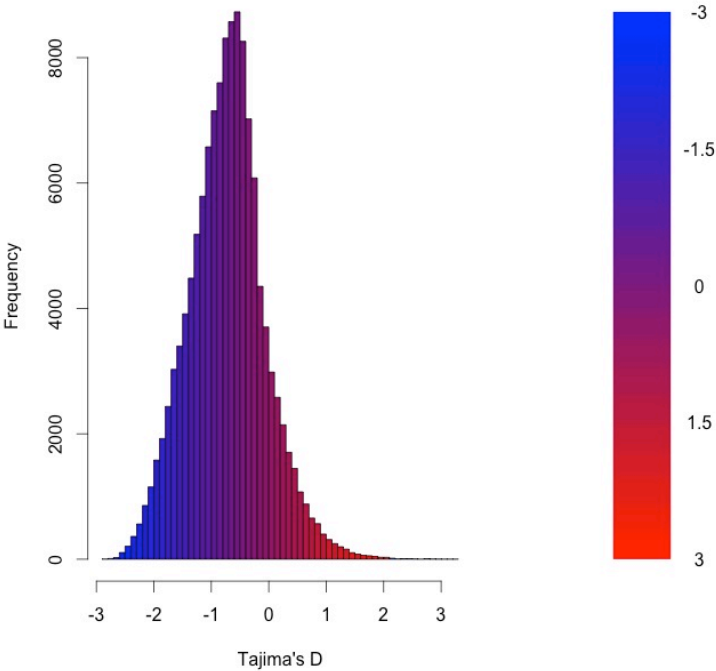
230

231 Figure 2. The distribution of Tajima's D for all putative transcripts.

232 **Table 3**

233

Transcript ID	GenBank ID	Description	Tajima's D
Transcript_49049	XM_006533884.1	heterogeneous nuclear ribonucleoprotein H1 (Hnrnph1)	3.26
Transcript_38378	XM_006522973.1	Son DNA binding protein (Son)	3.19
Transcript_126187	NM_133739.2	transmembrane protein 123 (Tmem123)	3.02
Transcript_70953	XM_006539066.1	chloride channel Kb (Clcnkb)	2.96
Transcript_37736	XM_006997718.1	h-2 class I histocompatibility antigen	2.92
Transcript_21448	XM_006986148.1	zinc finger protein 624-like	2.84
Transcript_47450	NM_009560.2 zinc	finger protein 60 (Zfp60)	2.82
Transcript_122250	XM_006539068.1	chloride channel Kb (Clcnkb)	2.81
Transcript_78367	XM_006496814.1	CDC42 binding protein kinase alpha (Cdc42bpa)	2.78
Transcript_96470	XM_006987129.1	interferon-inducible GTPase 1-like	2.77

Table 3. The 10 transcripts with the highest values for Tajima's D, which suggests balancing selection.

Table 4

Transcript ID	GenBank ID	Description	Tajima's D
Transcript_84359	XM_006991127.1	nuclear receptor coactivator 3 (Ncoa3)	-2.82
Transcript_87121	XM_006970128.1	methyl-CpG binding domain protein 2 (Mbd2)	-2.82
Transcript_125755	EU053203.1	alpha globin gene cluster	-2.78
Transcript_87128	XM_006976644.1	membrane-associated ring finger (March5)	-2.76
Transcript_55468	XM_006978377.1	Vpr binding protein (Vprbp)	-2.75
Transcript_116042	XM_006980811.1	membrane associated guanylate kinase (Magi3)	-2.75
Transcript_18966	XM_006982814.1	ubiquitin protein ligase E3 component n-recognin 5 (Ubr5)	-2.75
Transcript_122204	XM_008772511.1	zinc finger protein 612 (Zfp612)	-2.75
Transcript_100550	XM_006971297.1	bromodomain adjacent to zinc finger domain, 1B (Baz1b)	-2.74
Transcript_33267	XM_006975561.1	pumilio RNA-binding family member 1 (Pum1)	-2.75

Table 4. The 10 transcripts with the lowest values for Tajima's D, which suggests purifying or directional selection.

Natural Selection

To begin to test the hypothesis that selection on transcripts related to osmoregulation is enhanced in the desert adapted *P. eremicus*, we implemented the branch-site test as described above by setting the sequence corresponding to *P. eremicus* for both Slc2a9 and Vdr as the foreground lineages in 2 distinct program executions. These two transcripts were chosen specifically because they - the former significantly - were recently linked to osmoregulation in a desert

rodent [12]. The test for Slc2a9 was highly significant ($2\Delta\text{Lnl}=51.4$, df=1, p=0), indicating enhanced selection in *P. eremicus* relative to the other lineages. The branch site test for positive selection conducted on the Vdr gene was non-significant ($2\Delta\text{Lnl}=0.68$, df=1, p=1). This limited analysis of selection is to be followed up by an analysis of genome wide patterns of natural selection.

Conclusions

As a direct result of intense heat and aridity, deserts are thought to be amongst the harshest environments, particularly for mammalian inhabitants. Given that osmoregulation can be challenging for these animals - with failure resulting in death - strong selection should be observed on genes related to the maintenance of water and solute balance. This study aimed to characterize the transcriptome of a desert-adapted rodent species, *P. eremicus*. Specifically, we characterized the transcriptome of four tissue types (liver, kidney, brain, and testes) from a single individual and supplemented this with population-level renal transcriptome sequencing from 15 additional animals. We identified a set of transcripts undergoing both purifying and balancing selection based on Tajima's D. In addition, we used a branch site test to identify a transcript, likely related to desert osmoregulation, undergoing enhanced selection in *P. eremicus* relative to a set of non-desert rodents.

Acknowledgments

References

1. Walsberg G (2000) Small mammals in hot deserts: Some generalizations revisited. Bioscience 50: 109–120.

2. Tatum R, Zhang Y, Salleng K, Lu Z, Lin JJ, et al. (2009) Renal salt wasting and chronic dehydration in claudin-7-deficient mice. AJP: Renal Physiology 298: F24–F34.

3. Romero DG, Plonczynski MW, Welsh BL, Gomez-Sanchez CE, Zhou MY, et al. (2007) Gene expression profile in rat adrenal zona glomerulosa cells stimulated with aldosterone secretagogues. Physiological Genomics 32: 117–127.

4. Rojek A, Rojek A, Fuchtbauer E, Fuchtbauer E, Kwon T, et al. (2006) Severe urinary concentrating defect in renal collecting duct-selective AQP2 conditional-knockout mice.

15. Feng BJ, Sun LD, Soltani-Arabshahi R, Bowcock AM, Nair RP, et al. (2007) Toward a Molecular Phylogeny for *Peromyscus*: Evidence from Mitochondrial Cytochrome- b Sequences. Journal of Mammalogy 88: 1146–1159.

16. Shorter KR, Owen A, anderson V, Hall-South AC, Hayford S, et al. (2014) Natural genetic variation underlying differences in *Peromyscus* repetitive and social/aggressive behaviors. Behavior genetics 44: 126–135.

17. Panhuis TM, Broitman-Maduro G, Uhrig J, Maduro M, Reznick DN (2011) Analysis of Expressed Sequence Tags from the Placenta of the Live-Bearing Fish Poeciliopsis (Poeciliidae). Journal of Heredity 102: 352–361.

18. Shorter KR, Crossland JP, Webb D, Szalai G, Felder MR, et al. (2012) *Peromyscus* as a Mammalian Epigenetic Model. Genetics Research International 2012: 1–11.

19. Sikes RS, Gannon WL, Animal Care and Use Committee of the American Society of Mammalogists (2011) Guidelines of the American Society of Mammalogists for the use of wild mammals in research. Journal of Mammalogy 92: 235–253.

20. Heo Y, Wu XL, Chen D, Ma J, Hwu WM (2014) BLESS: Bloom filter-based error correction solution for high-throughput sequencing reads. Bioinformatics 30: 1354–1362.

21. MacManes MD (2014) On the optimal trimming of high-throughput mRNA sequence data. Frontiers in Genetics 5.

22. Mbandi SK, Hesse U, Rees DJG, Christoffels A (2014) A glance at quality score: Implication for *de novo* transcriptome reconstruction of Illumina reads. Frontiers in Genetics 5: 17.

23. Lohse M, Bolger AM, Nagel A, Fernie AR, Lunn JE, et al. (2012) RobiNA: A user-friendly, integrated software solution for RNA-Seq-based transcriptomics. Nucleic Acids Research 40: W622–7.

24. Haas BJ, Papanicolaou A, Yassour M, Grabherr M, Blood PD, et al. (2013) *De novo* transcript sequence reconstruction from RNA-seq using the Trinity platform for reference generation and analysis. Nature Protocols 8: 1494–1512.

25. **MacManes** MD, Lacey EA (2012) The Social Brain: Transcriptome Assembly and Characterization of the Hippocampus from a Social Subterranean Rodent, the Colonial Tuco-Tuco (*Ctenomys sociabilis*). PLOS ONE 7: e45524.

26. Li W, Godzik A (2006) Cd-hit: A fast program for clustering and comparing large sets of protein or nucleotide sequences. Bioinformatics 22: 1658–1659.

27. Camacho C, Coulouris G, Avagyan V, Ma N, Papadopoulos J, et al. (2009) BLAST+: architecture and applications. BMC Bioinformatics 10: 421.

28. Mi H (2004) The PANTHER database of protein families, subfamilies, functions and pathways. Nucleic Acids Research 33: D284–D288.

29. Wheeler TJ, Eddy SR (2013) nhmmer: DNA homology search with profile HMMs. Bioinformatics 29: 2487–2489.

30. Punta M, Coggill PC, Eberhardt RY, Mistry J, Tate J, et al. (2012) The Pfam protein families database. Nucleic Acids Research 40: D290–301.

31. Li H (2013) Aligning sequence reads, clone sequences and assembly contigs with BWA-MEM .

32. Roberts A, Pachter L (2013) Streaming fragment assignment for real-time analysis of sequencing experiments. Nature Methods 10: 71–73.

33. Korneliussen I Thorfinn Sand Moltke, Albrechtsen a, Nielsen R (2013) Calculation of Tajima's D and other neutrality test statistics from low depth next-generation sequencing data. BMC Bioinformatics 14: 289.

34. Ranwez V, Harispe S, Delsuc F, Douzery EJP (2011) MACSE: Multiple Alignment of Coding SEquences Accounting for Frameshifts and Stop Codons. PLOS ONE 6: e22594.

35. Aubry S, Kelly S, Kümpers BMC, Smith-Unna RD, Hibberd JM (2014) Deep Evolutionary Comparison of Gene Expression Identifies Parallel Recruitment of Trans-Factors in Two Independent Origins of C4 Photosynthesis. PLOS Genetics 10: e1004365.

36. Yang Z, dos Reis M (2011) Statistical Properties of the Branch-Site Test of Positive Selection. Molecular Biology and Evolution 28: 1217–1228.

37. Yang Z (2007) PAML 4: Phylogenetic Analysis by Maximum Likelihood. Molecular Biology and Evolution 24: 1586–1591.

38. Chamary JV, Parmley JL, Hurst LD (2006) Hearing silence: non-neutral evolution at synonymous sites in mammals. Nature Reviews Genetics 7: 98–108.